J|A|C|S
ARTICLES

Published on Web 10/20/2010

1,4-Addition of Lithium Diisopropylamide to Unsaturated Esters: Role of Rate-Limiting Deaggregation, Autocatalysis, Lithium Chloride Catalysis, and Other Mixed Aggregation Effects

Yun Ma, Alexander C. Hoepker, Lekha Gupta, Marc F. Faggin, and David B. Collum*

Department of Chemistry and Chemical Biology, Baker Laboratory, Cornell University, Ithaca, New York 14853-1301

Received July 2, 2010; E-mail: dbc6@cornell.edu

Abstract: Lithium diisopropylamide (LDA) in tetrahydrofuran at −78 °C undergoes 1,4-addition to an unsaturated ester via a rate-limiting deaggregation of LDA dimer followed by a post-rate-limiting reaction with the substrate. Muted autocatalysis is traced to a lithium enolate-mediated deaggregation of the LDA dimer and the intervention of LDA−lithium enolate mixed aggregates displaying higher reactivities than LDA. Striking accelerations are elicited by <1.0 mol % LiCl. Rate and mechanistic studies have revealed that the uncatalyzed and catalyzed pathways funnel through a common monosolvated-monomer-based intermediate. Four distinct classes of mixed aggregation effects are discussed.

Introduction

1,4-Additions of lithium amides have been reported on numerous occasions.[1−3] In one of the earliest reports, Schlessinger and co-workers found that attempted enolizations of unsaturated esters using lithium diisopropylamide (LDA) in tetrahydrofuran (THF) at −78 °C afforded β-amino esters instead.[1,4] They solved the problem by adding hexamethylphosphoramide (HMPA). Davies and co-workers, recognizing the medicinal importance of β-amino esters, developed highly enantioselective 1,4-additions of structurally analogous β-phenethylamine-derived lithium dialkylamides.[3]

Our interest was piqued by the 1,4-addition of LDA described in eq 1. Previous studies of the 1,4-addition in the presence of HMPA showed that addition occurs to the exclusion of enolization via highly solvated LDA dimers suggested to be triple ions.[5−7] When the reaction is carried out in the absence of HMPA under conditions that would be familiar to synthetic organic chemists (LDA/THF/−78 °C), strange decays are observed that are neither first- nor second-order (Figure 1, curve A). The near linearity of these decays seems more akin to a zeroth-order dependence on ester.[8,9] Moreover, traces of LiCl (<1 mol %) elicit a 70-fold acceleration accompanied by curvature that appears decidedly more normal (Figure 1, inset).

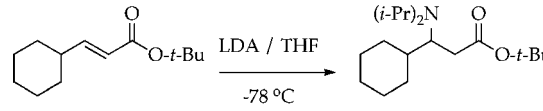

(1)

1 **2**

82% yield

We describe herein rate and mechanistic studies of the 1,4-addition in eq 1. The superposition of rate-limiting deaggregation, intervention of LDA−lithium enolate mixed aggregates, muted autocatalysis, and marked catalysis by LiCl presents considerable mechanistic complexity.[10] Such overt complexity is exhilarating in a mechanistic context, yet the growing number of examples of such odd effects affiliated with LDA/THF/−78 °C are troubling in light of the prevalence of these conditions in organic synthesis.[11,12] Furthermore, the LiCl catalysis, which is detectable using as little as 1.0 ppm LiCl, represents a mixed aggregation effect that is, to the best of our knowledge, undocumented.[13−15]

The Results describes strategies and tactics for specialists who wish to understand the details of the rate studies; the section

(1) (a) Herrman, J. L.; Kieczykowski, G. R.; Schlessinger, R. H. *Tetrahedron Lett.* **1973**, *14*, 2433. (b) Doi, H.; Sakai, T.; Iguchi, M.; Yamada, K.; Tomioka, K. *J. Am. Chem. Soc.* **2003**, *125*, 2886. (c) Uyehara, T.; Asao, N.; Yamamoto, Y. *J. Chem. Soc., Chem. Commun.* **1987**, 1410. (d) Amputch, M. A.; Matamoros, R.; Little, R. D. *Tetrahedron* **1994**, *50*, 5591. (e) Hase, T. A.; Kukkola, P. *Synth. Commun.* **1980**, *10*, 451. (f) Inokuchi, T.; Kawafuchi, H. *J. Org. Chem.* **2007**, *72*, 1472.

(2) Bellasoued, M.; Ennigrou, R.; Gaudemar, M. *J. Organomet. Chem.* **1988**, *338*, 149.

(3) Davies, S. G.; Smith, A. D.; Price, P. D. *Tetrahedron: Asymmetry* **2005**, *16*, 2833.

(4) (a) Bakker, W. I. I.; Wong, P. L.; Snieckus, V. Lithium Diisopropylamide. In *e-EROS*; Paquette, L. A., Ed.; Wiley: New York, 2001. (b) Clayden, J. *Organolithiums: Selectivity for Synthesis*; Baldwin, J. E., Williams, R. M., Eds.; Pergamon Press: New York, 2002.

(5) Ma, Y.; Collum, D. B. *J. Am. Chem. Soc.* **2007**, *129*, 14818.

(6) For a review summarizing rate studies of LDA-mediated reactions, see: Collum, D. B.; McNeil, A. J.; Ramirez, A. *Angew. Chem., Int. Ed.* **2007**, *46*, 3002.

(7) For an attempted comprehensive bibliography of triple ions of lithium salts, see: Ma, Y.; Ramirez, A.; Singh, K. J.; Keresztes, I.; Collum, D. B. *J. Am. Chem. Soc.* **2006**, *128*, 15399.

(8) (a) Espenson, J. H. *Chemical Kinetics and Reaction Mechanisms*, 2nd ed.; McGraw-Hill: New York, 1995; Chapter 2, p 44. Atkins, P. W.; Jones, L. L. *Chemical Principles: The Quest for Insight*, 2nd ed.; W. H. Freeman: New York, 2002.

10.1021/ja105855v

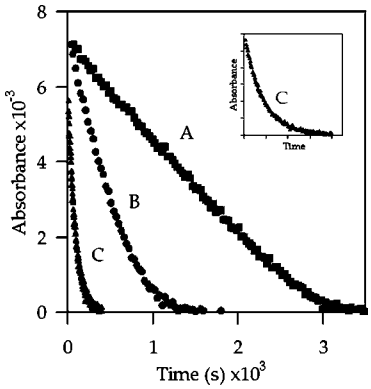

Figure 1. Plot of IR absorbance vs time in THF (6.10 M) for 1,4-addition of ester **1** (0.004 M) with LDA (0.10 M) at −78 °C in the presence of various amounts of LiCl: (A) no LiCl; (B) 0.01 mol % LiCl; (C) 0.4 mol % LiCl. The inset shows an expanded view of curve C.

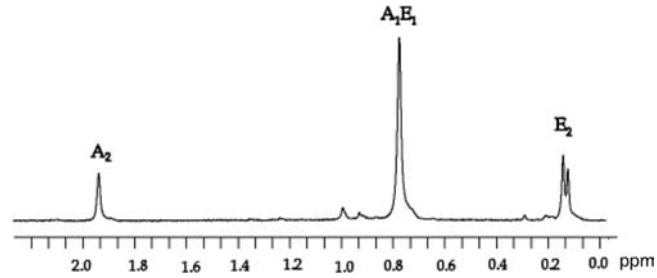

Figure 2. Representative ^{6}Li NMR spectrum of a 60:40 mixture of [^{6}Li]**5** and [^{6}Li]**3** showing resonances of the homodimers (A_2 and E_2) and the mixed dimer [^{6}Li]**4** (AE).

culminates in a mechanistic hypothesis that accounts for the disparate behaviors. The Discussion summarizes the results for a more general audience and describes how mixed aggregates influence the reactivity.

Results

Caveat: Purification of LDA. We previously showed by potentiometry[16] and ion chromatography[17] that recrystallized LDA[18] prepared from recrystallized *n*-BuLi[19] contains <0.02 mol % LiCl.[11,12] Accelerations of the 1,4-addition in eq 1 by as little as *0.001 mol % LiCl*, however, prompted us to modify a literature synthesis[20] of rigorously LiCl-free LDA from lithium metal, diisopropylamine, isoprene, and dimethylethylamine (DMEA). DMEA accelerates the reduction yet does not remain bound to the recrystallized LDA.[21] Despite taking these precautions, however, we observed some variability when stock solutions prepared from a common batch of LDA were used. Control experiments examining the influence of LDA aging, traces of H_2O and O_2, contaminants in solvents, joint greases, and even the specific researcher carrying out the work failed to uncover the source of this residual variability. The consequences were not large, although triplicate measurements proved necessary in some instances.

Solution Structures. Reaction of 2.0 equiv of LDA with unsaturated ester **1** in THF at −78 °C with slow warming to room temperature afforded β-amino ester **2** in 82% yield (eq 1).[5] Monitoring the reaction of [^{6}Li,^{15}N]LDA with ester **1** using ^{6}Li and ^{15}N NMR spectroscopy revealed the presence of LDA−lithium enolate mixed dimer **4** along with a concentration-independent pair of resonances in a nearly 1:1 ratio that was shown by the absence of ^{6}Li−^{15}N coupling to be attributable to enolate **5** (Figure 2). Although we were tempted to presume that the two resonances derived from an *E*/*Z* mixture, we suspected that they were homochiral and heterochiral dimers **5a**. (The existence of chelation is depicted out of convenience; the typically small Li−N coupling anticipated for a Li−NR_3 interaction[22] was not observed.) By varying the proportions of LDA and lithium enolate and monitoring LDA homodimer **3**, mixed dimer **4**, and the enolate homoaggregates (an A_2−AE−E_n ensemble), we used the method of continuous variation (the method of Job[23]) to show that the enolate (E_n) is indeed a dimer (Figure 3). Detailed descriptions of this method for characterizing lithium enolates have been reported.[24] Although mono-

(9) For other examples of odd linearities that may or may not have origins similar to those described herein, see: (a) Blackmond, D. G.; Ropic, M.; Stefinovic, M. *Org. Process Res. Dev.* **2006**, *10*, 457. (b) Akao, A.; Nonoyama, N.; Mase, T.; Yasuda, N. *Org. Process Res. Dev.* **2006**, *10*, 1178. (c) Rowley, J. M.; Lobkovsky, E. B.; Coates, G. W. *J. Am. Chem. Soc.* **2007**, *129*, 4948. (d) Yin, C.-X.; Finke, R. G. *J. Am. Chem. Soc.* **2005**, *127*, 13988.

(10) For examples of reactions that are fast relative to aggregate−aggregate exchanges, see: (a) McGarrity, J. F.; Ogle, C. A. *J. Am. Chem. Soc.* **1985**, *107*, 1810. (b) Jones, A. C.; Sanders, A. W.; Bevan, M. J.; Reich, H. J. *J. Am. Chem. Soc.* **2007**, *129*, 3492. (c) Thompson, A.; Corley, E. G.; Huntington, M. F.; Grabowski, E. J. J.; Remenar, J. F.; Collum, D. B. *J. Am. Chem. Soc.* **1998**, *120*, 2028. (d) Jones, A. C.; Sanders, A. W.; Sikorski, W. H.; Jansen, K. L.; Reich, H. J. *J. Am. Chem. Soc.* **2008**, *130*, 6060. (e) Reference 11.

(11) Singh, K. J.; Hoepker, A. C.; Collum, D. B. *J. Am. Chem. Soc.* **2008**, *130*, 18008.

(12) Gupta, L.; Hoepker, A. C.; Singh, K. J.; Collum, D. B. *J. Org. Chem.* **2009**, *74*, 2231.

(13) For leading references and discussions of mixed aggregation effects, see: (a) Seebach, D. *Angew. Chem., Int. Ed. Engl.* **1988**, *27*, 1624. (b) Tchoubar, B.; Loupy, A. *Salt Effects in Organic and Organometallic Chemistry*; VCH: New York, 1992; Chapters 4, 5, and 7. (c) Briggs, T. F.; Winemiller, M. D.; Xiang, B.; Collum, D. B. *J. Org. Chem.* **2001**, *66*, 6291. (d) Caubère, P. *Chem. Rev.* **1993**, *93*, 2317.

(14) Seebach, D. In *Proceedings of the Robert A. Welch Foundation Conferences on Chemistry and Biochemistry*; Wiley: New York, 1984; p 93.

(15) Ramirez, A.; Sun, X.; Collum, D. B. *J. Am. Chem. Soc.* **2006**, *128*, 10326, and references cited therein.

(16) Evans, A. *Potentiometry and Ion-Selective Electrodes*; Wiley: New York, 1987.

(17) Fuji, T. *Anal. Chem.* **1992**, *64*, 775.

(18) Kim, Y.-J.; Bernstein, M. P.; Galiano-Roth, A. S.; Romesberg, F. E.; Fuller, D. J.; Harrison, A. T.; Collum, D. B.; Williard, P. G. *J. Org. Chem.* **1991**, *56*, 4435.

(19) Kottke, T.; Stalke, D. *Angew. Chem., Int. Ed. Engl.* **1993**, *32*, 580. Rennels, R. A.; Maliakal, A. J.; Collum, D. B. *J. Am. Chem. Soc.* **1998**, *120*, 421.

(20) (a) Marck, W.; Huisgen, R. *Chem. Ber.* **1960**, *93*, 608. (b) Gaudemar-Bardone, F.; Gaudemar, M. *Synthesis* **1979**, 463. (c) Reetz, M. T.; Maier, W. F. *Liebigs Ann. Chem.* **1980**, 1471. (d) Williard, P. G.; Carpenter, G. B. *J. Am. Chem. Soc.* **1986**, *108*, 462. Williard, P. G.; Salvino, J. M. *J. Org. Chem.* **1993**, *58*, 1. (e) Morrison, R. C.; Hall, R. W.; Rathman, T. L. Stable Lithium Diisopropylamide and Method of Preparation. U.S. Patent 4,595,779, June 17, 1986.

(21) See: Zhao, P.; Collum, D. B. *J. Am. Chem. Soc.* **2003**, *125*, 14411, and references cited therein.

(22) Lucht, B. L.; Collum, D. B. *J. Am. Chem. Soc.* **1996**, *118*, 3529. Waldmüller, D.; Kotsatos, B. J.; Nichols, M. A.; Williard, P. G. *J. Am. Chem. Soc.* **1997**, *119*, 5479. Sato, D.; Kawasaki, H.; Shimada, I.; Arata, Y.; Okamura, K.; Date, T.; Koga, K. *J. Am. Chem. Soc.* **1992**, *114*, 761. Reich, H. J.; Goldenberg, W. S.; Gudmundsson, B. O.; Sanders, A. W.; Kulicke, K. J.; Simon, K.; Guzei, I. A. *J. Am. Chem. Soc.* **2001**, *123*, 8067. Johansson, A.; Davidsson, O. *Chem.—Eur. J.* **2001**, *7*, 3461. Aubrecht, K. B.; Lucht, B. L.; Collum, D. B. *Organometallics* **1999**, *18*, 2981.

(23) Job, P. *Ann. Chim.* **1928**, *9*, 113. For more recent examples and leading references, see: Huang, C. Y. *Methods Enzymol.* **1982**, *87*, 509. Hubbard, R. D.; Horner, S. R.; Miller, B. L. *J. Am. Chem. Soc.* **2001**, *123*, 5810. Potluri, V.; Maitra, U. *J. Org. Chem.* **2000**, *65*, 7764.

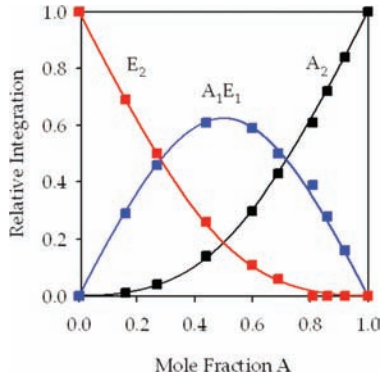

Figure 3. Plot of the relative integrations of [^{6}Li]**3** (A_2), [^{6}Li]**4** (AE), and [^{6}Li]**5** (E_2) vs the mole fraction of LDA (A). The curves were derived from a parametric fit as described previously.[24]

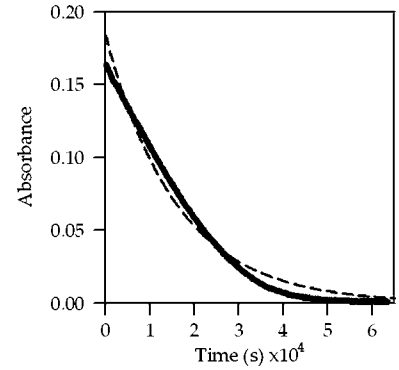

Figure 4. Plot showing IR absorbance of ester **1** vs time for the 1,4-addition of ester **1** (0.10 M) with LDA (0.10 M) in neat THF at −78 °C. The dashed line shows the poor first-order fit ($A = ae^{bt}$).

meric enolate was not observed, it is invoked as an intermediate. Density functional theory (DFT) computations at the B3LYP/6-31G(d) level of theory[25] suggested disolvated monomer **5b** as the fleetingly stable resting state.

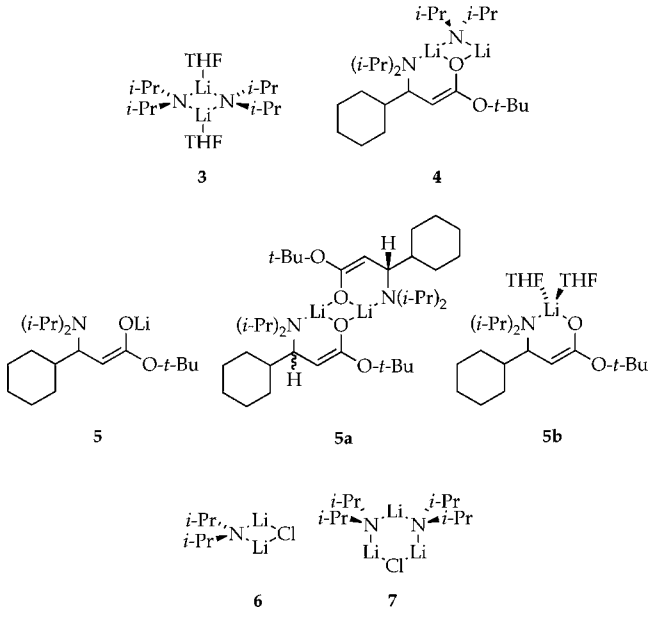

Catalysis by LiCl is discussed in light of the structures of LDA−LiCl mixed aggregates. Previous studies have shown that LiCl is dimeric in THF solution.[26,27] Mixtures of LDA with LiCl at the very low LiCl concentrations used in the rate studies described below (≤2 mol % LiCl) afford a LiCl-concentration-independent 1:8 mixture of **6** and **7** to the exclusion of free LiCl.[27,28]

Kinetics: General Protocols. LDA used in rate studies was prepared as described above. Exogenous LiCl was generated in situ from $Et_3N \cdot HCl$.[29] (The Et_3N byproduct is a poor ligand[21] that has no effect on LDA structure or reactivity.) The disappearance of ester **1** (1715 cm^{-1}) during the 1,4-additions was monitored using in situ IR spectroscopy.[30] Formation of lithium enolate **5** (1630 cm^{-1}) was correlated with the loss of **1**. It should be noted, however, that the absorbance at 1630 cm^{-1} arises from the superposition of mixed and homoaggregated dimers **4** and **5a**, respectively. Using ^{6}Li NMR spectroscopy, we were able to show that this IR spectral simplicity belies a substantial underlying complexity (see below).[31]

Strange Curvatures. Monitoring addition of LDA to ester **1** by IR spectroscopy under pseudo-first-order conditions (excess LDA) showed a linear decay, suggesting a zeroth-order dependence on ester **1**. Equimolar mixtures of LDA and ester **1** (second-order conditions) afforded the decay depicted in Figure 4. If the linearity in Figure 1 derived solely from a zeroth-order dependence on ester **1**, this dependence in conjunction with a first-order dependence on LDA would cause the decay in Figure 4 to be first-order overall. The first-order fit in Figure 4 (dashed line) is poor, suggesting a persistent linearity stemming from autocatalysis (see below). (Previous studies of arylcarbamate lithiations revealed linear decays that were traced to straightening of first-order decays by autocatalysis.[11])

^{6}Li NMR spectroscopy allowed us to follow the loss of LDA dimer **3**, mixed dimer **4**, and enolate dimer **5a** (Figure 5). The concentrations of the aggregates also allowed us to calculate the concentration of the spectroscopically silent ester **1**. The calculated linear decay of ester **1** correlated well with the experimentally measured linear decay detected by IR spectroscopy. The curved loss of LDA dimer **3** (the noncorrelation with

(24) (a) Liou, L. R.; McNeil, A. J.; Ramirez, A.; Toombes, G. E. S.; Gruver, J. M.; Collum, D. B. *J. Am. Chem. Soc.* **2008**, *130*, 4859. (b) Gruver, J. M.; Liou, L. R.; McNeil, A. J.; Ramirez, A.; Collum, D. B. *J. Org. Chem.* **2008**, *73*, 7743.
(25) Frisch, M. J.; et al. *Gaussian 03*, revision B.04; Gaussian, Inc.: Wallingford, CT, 2004.
(26) (a) Reich, H. J.; Borst, J. P.; Dykstra, R. R.; Green, D. P. *J. Am. Chem. Soc.* **1993**, *115*, 8728. (b) Wong, M. K.; Popov, A. I. *J. Inorg. Nucl. Chem.* **1972**, *34*, 3615. (c) Yakimansky, A. V.; Müller, A. H.; Beylen, M. V. *Macromolecules* **2000**, *33*, 5686. (d) Goralski, P.; Chabanel, M. *Inorg. Chem.* **1987**, *26*, 2169, and references cited therein.
(27) Studies of LDA−LiCl at ultralow LiCl concentrations as well as confirmation of LiCl in THF as a dimer will be reported in due course.
(28) Galiano-Roth, A. S.; Kim, Y.-J.; Gilchrist, J. H.; Harrison, A. T.; Fuller, D. J.; Collum, D. B. *J. Am. Chem. Soc.* **1991**, *113*, 5053. Also see: Hall, P. L.; Gilchrist, J. H.; Collum, D. B. *J. Am. Chem. Soc.* **1991**, *113*, 9571.
(29) Snaith and coworkers underscored the merits of R_3NHX salts as precursors to anhydrous LiX salts. See: Barr, D.; Snaith, R.; Wright, D. S.; Mulvey, R. E.; Wade, K. *J. Am. Chem. Soc.* **1987**, *109*, 7891. Also see: Hall, P. L.; Gilchrist, J. H.; Collum, D. B. *J. Am. Chem. Soc.* **1991**, *113*, 9571.
(30) Rein, A. J.; Donahue, S. M.; Pavlosky, M. A. *Curr. Opin. Drug Discovery Dev.* **2000**, *3*, 734.
(31) Addition of excess *i*-Pr_2NH to the metalation had no measurable effect on the rates or curvatures.

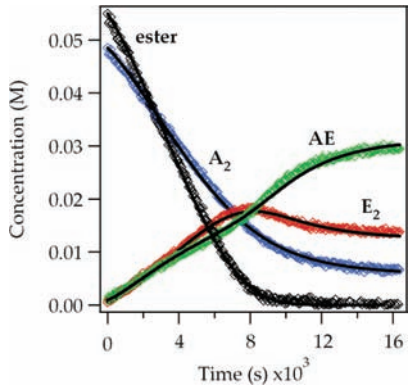

Figure 5. Time-dependent concentrations measured by ^{6}Li NMR spectroscopy using 0.05 M **3** (0.10 N) and 0.05 M **1** in 6.1 M THF at −78 °C. Legend: ester = **1**; A_2 = LDA dimer **3**; E_2 = enolate dimer **5a**; AE = enolate mixed dimer **4**. The curves represent a parametric fit to eqs 17−22 (described below). The best-fit values for the rate constants are listed in the Supporting Information.

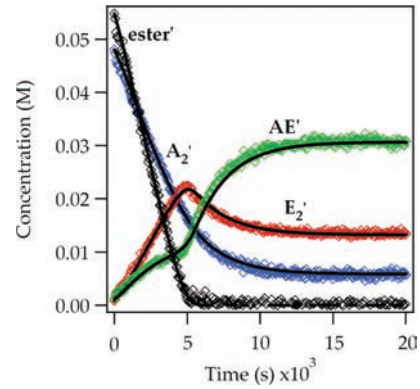

Figure 7. Time-dependent concentrations measured by ^{6}Li NMR spectroscopy using 0.05 M **3** (0.10 N) and 0.05 M ester **12** in 6.1 M THF at −78 °C. Legend: ester = **12**; A_2 = LDA dimer **3**; E_2' = enolate dimer of ester **12**; AE′ = enolate mixed dimer. The curves represent a parametric fit to eqs 17−22 (described below). The best-fit values for the rate constants are listed in the Supporting Information.

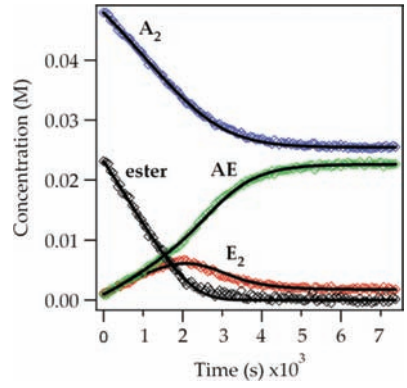

Figure 6. Time-dependent concentrations measured by ^{6}Li NMR spectroscopy using 0.05 M **3** (0.10 N) and 0.025 M **1** in 6.1 M THF at −78 °C. Legend: ester = **1**; A_2 = LDA dimer **3**; E_2 = enolate dimer **5a**; AE = enolate mixed dimer **4**. The curves represent a parametric fit to eqs 17−22 (described below). The best-fit values for the rate constants are listed in the Supporting Information.

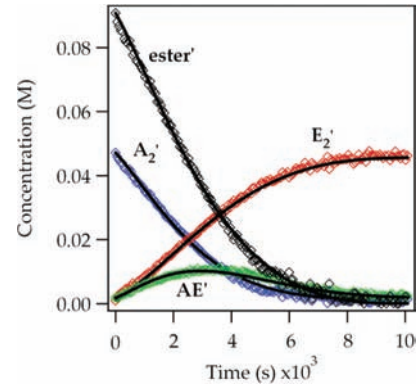

Figure 8. Time-dependent concentrations measured by ^{6}Li NMR spectroscopy using 0.05 M **3** (0.10 N) and 0.10 M **12** in 6.1 M THF at −78 °C. Legend: ester = **12**; A_2 = LDA dimer **3**; E_2' = enolate dimer of **12**; AE′ = enolate mixed dimer. The curves represent a parametric fit to eqs 17−22 (described below). The best-fit values for the rate constants are listed in the Supporting Information.

the ester) reflects the consumption of **3** by both metalation and formation of mixed dimer **4**. The time dependencies of **4** and **5a** (represented as AE and E_2 in Figures 5 and 6) clearly departed from conventional behavior. Minor changes in the initial concentration of ester **1** produced overt visual changes (Figure 6). Even more striking curvatures and discontinuities were observed when *n*-alkyl ester **12** was used (Figures 7 and 8). (Ester **12**, *n*-$C_7H_{15}CH{=}CHCO_2$-*t*-Bu, was introduced in the context of the competition studies described below.) The overshoot of the concentration of enolate dimer **5a** relative to the final equilibrium value and the discontinuity in the mixed dimer concentration place significant constraints on a mechanistic model. The rate studies described below were employed to extract the critical details required to account for the strange time-dependent concentrations, and best-fit numerical integrations afforded the curves (see below).

Kinetics: Uncatalyzed 1,4-Additions. The mechanism of the uncatalyzed 1,4-addition (i.e., the addition before the appearance of mixed dimers and the onset of autocatalysis) was examined by monitoring the rates at early conversion using IR spectroscopy. Plots of ester concentration versus time for different initial concentrations of ester **1** (Figure 9) showed linear, parallel decays consistent with a zeroth-order dependence on **1**, which was confirmed by a plot of the initial rates versus initial ester concentration (Figure 10). Plots of initial rate versus LDA concentration (Figure 11)[32] and THF concentration (Figure 12) revealed first-order dependencies in both instances. The ideal-

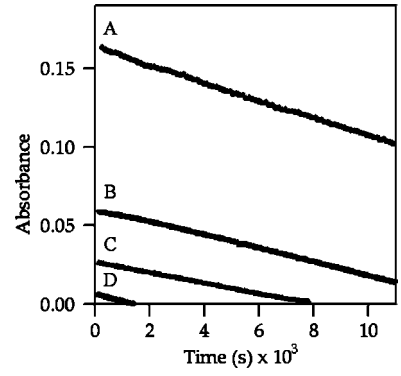

Figure 9. Plots of IR absorbance of ester **1** vs time for selected initial concentrations of **1**: (A) 0.10 M; (B) 0.050 M; (C) 0.025 M; (D) 0.004 M.

(32) The concentration of LDA, although expressed in units of molarity, refers to the concentration of the monomer unit (normality).

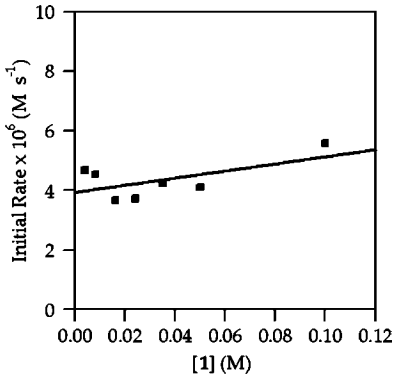

Figure 10. Plot of initial rate vs [**1**] in THF (6.1 M) for the 1,4-addition of ester **1** with LDA (0.10 M) at −78 °C. The curve depicts an unweighted least-squares fit to $y = k[\mathbf{1}] + k'$ [$k = (1.2 \pm 1) \times 10^{-5}$; $k' = (3.9 \pm 0.4) \times 10^{-6}$].

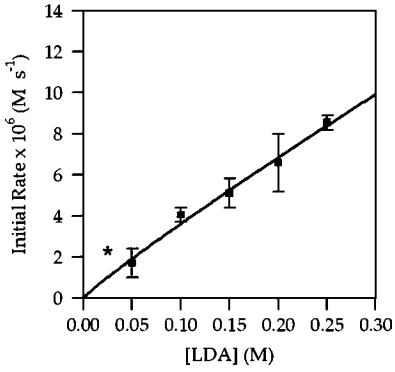

Figure 11. Plot of initial rate vs [LDA] in THF (6.10 M) for the 1,4-addition of ester **1** (0.004 M) at −78 °C. The curve depicts an unweighted least-squares fit to $y = k[\mathrm{LDA}]^n$ [$k = (3.1 \pm 0.4) \times 10^{-5}$; $n = 0.92 \pm 0.03$].

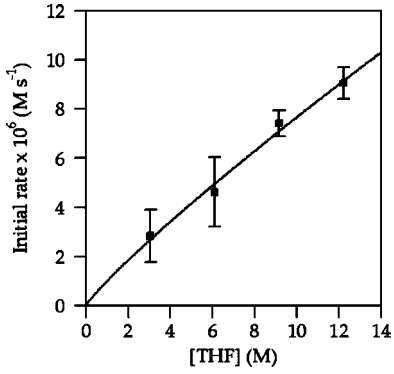

Figure 12. Plot of initial rate vs [THF] in hexane cosolvent for the 1,4-addition of ester **1** (0.004 M) with LDA (0.10 M) at −78 °C. The curve depicts an unweighted least-squares fit to $y = k[\mathrm{THF}]^n + k'$ [$k = (8.1 \pm 0.2) \times 10^{-7}$; $n = 0.95 \pm 0.03$; $k' = (4.05 \pm 0.04) \times 10^{-7}$].

ized[33] rate law given by eq 2 is consistent with a mechanism involving rate-limiting deaggregation (eq 3) followed by post-rate-limiting reaction with ester **1**.[34] To describe some fairly complex mechanistic scenarios, we take the liberty of introducing the following shorthand: A = an LDA monomeric subunit and S = THF (e.g., A_2S_2 = **3**).

$$-\frac{d[\mathbf{1}]}{dt} = k[A_2S_2][S] \quad (2)$$

$$A_2S_2 + S \xrightarrow{k} [A_2S_3]^{\ddagger} \quad (3)$$

Scheme 1

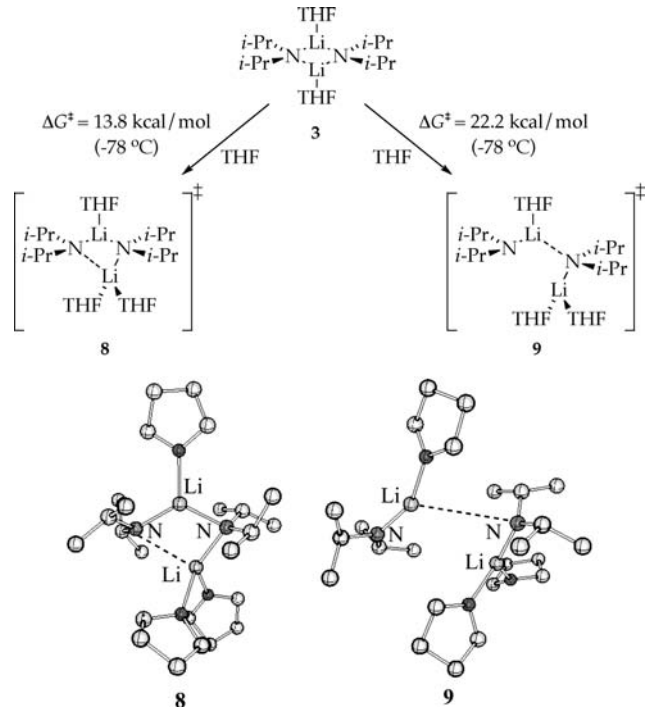

DFT computations showed that trisolvated-dimer-based transition structures representing rate-limiting open dimer formation (**8**) and deaggregation (**9**) are both plausible (Scheme 1).[35] The dimer-based rate-limiting step does *not* attest to whether the post-rate-limiting 1,4-addition is monomer- or dimer-based, but strong support for a monomer-based 1,4-addition emerged from studies of catalysis (see below).

Autocatalysis. Product-derived acceleration—so-called autocatalysis—in its most extreme form manifests sigmoidal decays of substrate versus time[36,37] and should be most easily observed

(33) We define the idealized rate law as that obtained by rounding the observed reaction orders to the nearest rational order.

(34) The rate law provides the stoichiometry of the transition structure relative to that of the reactants. See: Edwards, J. O.; Greene, E. F.; Ross, J. *J. Chem. Educ.* **1968**, *45*, 381.

(35) Open dimers were first proposed for the isomerization of oxiranes to allylic alcohols by mixed-metal bases. See: Mordini, A.; Rayana, E. B.; Margot, C.; Schlosser, M. *Tetrahedron* **1990**, *46*, 2401. For a bibliography of lithium amide open dimers, see ref 15.

(36) (a) Besson, C.; Finney, E. E.; Finke, R. G. *J. Am. Chem. Soc.* **2005**, *127*, 8179. (b) Besson, C.; Finney, E. E.; Finke, R. G. *Chem. Mater.* **2005**, *17*, 4925. (c) Huang, K. T.; Keszler, A.; Patel, N.; Patel, R. P.; Gladwin, M. T.; Kim-Shapiro, D. B.; Hogg, N. *J. Biol. Chem.* **2005**, *280*, 31126. (d) Huang, Z.; Shiva, S.; Kim-Shapiro, D. B.; Patel, R. P.; Ringwood, L. A.; Irby, C. E.; Huang, K. T.; Ho, C.; Hogg, N.; Schechter, A. N.; Gladwin, M. T. *J. Clin. Invest.* **2005**, *115*, 2099. (e) Tanj, S.; Ohno, A.; Sato, I.; Soai, K. *Org. Lett.* **2001**, *3*, 287. (f) Barrios-Landeros, F.; Carrow, B. P.; Hartwig, J. F. *J. Am. Chem. Soc.* **2008**, *130*, 5842.

(37) (a) Depue, J. S.; Collum, D. B. *J. Am. Chem. Soc.* **1988**, *110*, 5524. (b) McNeil, A. J.; Toombes, G. E. S.; Gruner, S. M.; Lobkovsky, E.; Collum, D. B.; Chandramouli, S. V.; Vanasse, B. J.; Ayers, T. A. *J. Am. Chem. Soc.* **2004**, *126*, 16559. (c) Nudelman, N. S.; Velurtas, S.; Grela, M. A. *J. Phys. Org. Chem.* **2003**, *16*, 669. (d) Alberts, A. H.; Wynberg, H. *J. Am. Chem. Soc.* **1989**, *111*, 7265. (e) Alberts, A. H.; Wynberg, H. *J. Chem. Soc., Chem. Commun.* **1990**, 453.

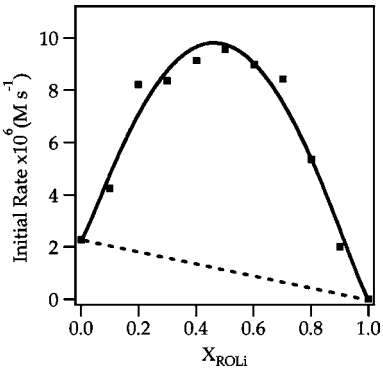

Figure 13. Plot of initial rate versus mole fraction of enolate (X_{ROLi}) for the serial injection of 10 aliquots of ester **1** (10 mol % each relative to LDA) into 0.10 M LDA in 6.1 M THF/hexane cosolvent at −78 °C. The dashed line depicts the theoretical behavior of the initial rate in the absence of autocatalysis, and the solid curve represents a nonlinear least-squares fit to eq 4.

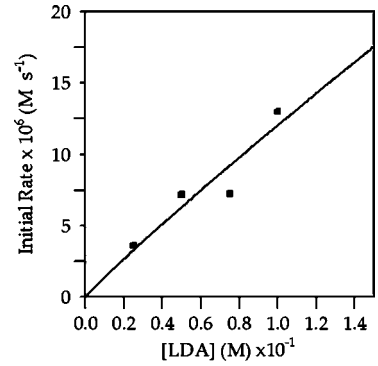

Figure 14. Plot of initial rate vs [LDA] for the condensation of LDA dimer **3** with enolate dimer **5a** (0.025 M) in THF (6.10 M) at −78 °C. The curve depicts an unweighted least-squares fit to $y = k[\mathrm{LDA}]^n$ [$k = (1.0 \pm 0.3) \times 10^{-4}$; $n = 0.93 \pm 0.24$].

using equimolar mixtures of LDA and substrate. Figure 1 shows no sigmoid but does show a persistent linearity in the first two half-lives, suggesting muted autocatalysis. We developed a method for detecting low levels of mixed aggregation effects using serial substrate injections as follows.

In a routine control experiment, the IR baseline was zeroed at the end of a pseudo-first-order kinetic run, and a second aliquot of substrate was added. In the absence of autocatalysis, the rate for the second aliquot should have shown a minor decrease relative to the first aliquot because of the slight loss in LDA titer. In the 1,4-addition, however, the second aliquot afforded a measurably *higher* rate. This effect was amplified by serially injecting aliquots containing 10 mol % ester **1** until the LDA was completely consumed. The initial rate is plotted versus mole fraction of enolate **5** (X_{ROLi}) in Figure 13. The serial injections correspond to movement from left to right along the X_{ROLi} axis.[23] Figure 13 differs from a standard plot of concentration versus time in that (1) the normal upward curvature resulting from substrate loss was factored out by adding substrate at constant concentrations and monitoring initial rates and (2) all aggregates were allowed to equilibrate between injections.

The maximum at $X_{ROLi} = 0.5$ in Figure 13 suggests that a 1:1 LDA/enolate ratio is optimal.[23,24] The solid curve in Figure 13 corresponds to a nonlinear least-squares fit to eq 4:

$$-\left.\frac{\Delta[\mathrm{ester}]}{\Delta t}\right|_{t=0} = k[X_{ROLi}]^n[1 - X_{ROLi}]^m + k'[1 - X_{ROLi}]^{1.0} \qquad (4)$$

(see the Supporting Information). This behavior could arise either from a key condensation involving LDA dimer **3** and enolate dimer **5a** (affording the mathematically equivalent 2:2 stoichiometry) or from mixed dimer **4** maximized at $X_{ROLi} = 0.5$. There is, however, a telling paradox: Figure 13 suggests that a 1,4-addition from equimolar mixtures of LDA and ester **1** should be markedly faster at 50% conversion than at the start. Nonetheless, there is no sigmoidal behavior in Figure 4; only a gentle straightening of the decay appears. (Perfect linearity arises when the autocatalysis precisely offsets the consumption of LDA.[11])

Using ^{6}Li NMR spectroscopy, we monitored the reaction of LDA dimer **3** and enolate dimer **5a** to give mixed dimer **4**. The reaction using 0.05 M each of **3** and **5a** revealed a half-life of 3000 s. First-order dependencies in **3** and **5a** (Figures 14 and 15) in conjunction with a zeroth-order THF dependence (see the Supporting Information) afforded the idealized[33] rate law given in eq 5:

$$-\frac{\mathrm{d}[\mathbf{1}]}{\mathrm{d}t} = k[A_2S_2][E_2][S]^0 \qquad (5)$$

The associative mechanism suggests mixed-tetramer-based exchange.[38] We can imagine ladder-based intermediates (eq 6),[39,40] but monomeric LDA would not necessarily be formed during the exchange, and the role this exchange plays in the 1,4-addition is minor at best (see below).[41]

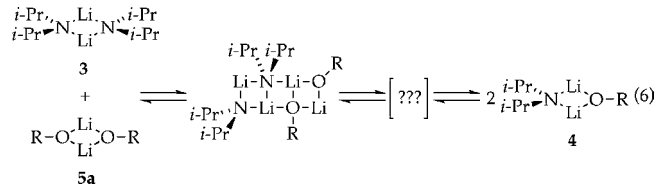

(6)

LiCl-Catalyzed 1,4-Additions. Very low concentrations of LiCl (<0.5 mol % relative to LDA) cause marked accelerations of the 1,4-addition and impart upward curvatures in plots of ester concentration versus time (Figure 1), which suggests that LiCl catalysis brings ester **1** into the rate law. The decays become cleanly first-order at >0.5 mol % LiCl under pseudo-first-order conditions. Plotting the initial rate versus LiCl concentration revealed saturation kinetics with rates that plateau at >0.5 mol % LiCl (Figure 16).[42]

Saturation often arises when a bimolecular reaction at low concentration becomes unimolecular at higher concentrations

(38) Tetramer-based intermediates have also been implicated in LDA-mediated ortholithiations. See: Ma, Y.; Hoepker, A. C.; Gupta, L.; Collum, D. B. Unpublished work.

(39) A four-rung LDA/enolate ladder structure has been characterized crystallographically. See: Williard, P. G.; Hintze, M. J. *J. Am. Chem. Soc.* **1987**, *109*, 5539.

(40) (a) Gregory, K.; Schleyer, P. v. R.; Snaith, R. *Adv. Inorg. Chem.* **1991**, *37*, 47. (b) Mulvey, R. E. *Chem. Soc. Rev.* **1991**, *20*, 167. (c) Beswick, M. A.; Wright, D. S. In *Comprehensive Organometallic Chemistry II*; Abels, E. W., Stone, F. G. A., Wilkinson, G., Eds.; Pergamon Press: New York, 1995; Vol. 1, Chapter 1. (d) Mulvey, R. E. *Chem. Soc. Rev.* **1998**, *27*, 339. (e) Rutherford, J. L.; Collum, D. B. *J. Am. Chem. Soc.* **1999**, *121*, 10198.

(41) (a) Paté, F.; Gérard, H.; Oulyadi, H.; de la Lande, A.; Harrison-Marchand, A.; Parisel, O.; Maddaluno, J. *Chem. Commun.* **2009**, 319. (b) Arvidsson, P. I.; Ahlberg, P.; Hilmersson, G. *Chem.—Eur. J.* **1999**, *5*, 1348.

(42) Saturation was also apparent when the observed rate constants from fits to the exponential decays were plotted.

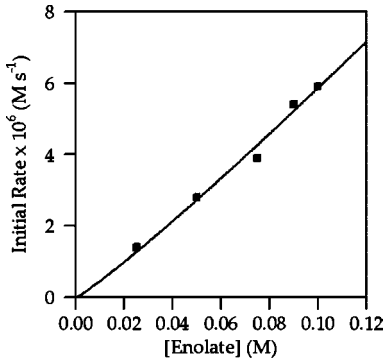

Figure 15. Plot of initial rate vs the concentration of enolate **5** for the condensation of LDA dimer **3** (0.10 M) with enolate dimer **5a** in THF (6.10 M) at −78 °C. The curve depicts an unweighted least-squares fit to $y = k[\text{enolate}]^n$ [$k = (7.4 \pm 0.3) \times 10^{-5}$; $n = 1.10 \pm 0.14$].

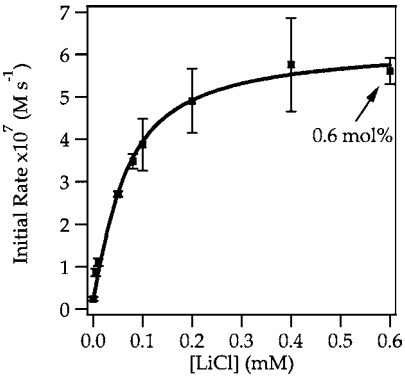

Figure 16. Plot of initial rate vs [LiCl] in THF (6.1 M) for the 1,4-addition of ester **1** (0.004 M) with LDA (0.10 M) at −78 °C. The 0.6 mol % notation is relative to the LDA concentration.

because an observable complex is formed.[43] Enzymology offers a plethora of examples under the rubric of Michaelis−Menten kinetics.[44] A Michaelis−Menten-like saturation behavior, however, would require ≥100 mol % LiCl, not a mere 0.5 mol %, to form observable LDA−LiCl mixed aggregates **6** and **7** as the dominant species.[45]

Saturation kinetics can also be caused by a change in the rate-limiting step.[43] Indeed, our rate studies are consistent with a scenario in which LiCl catalyzes a dimer−monomer exchange (eq 7):

$$^1/_2A_2S_2 \underset{k_{-1}[\text{LiCl}_T]}{\overset{k_1[\text{LiCl}_T]}{\rightleftharpoons}} \text{AS} \qquad (7)$$

where LiCl_T = lithium chloride titer. The competition studies described below confirmed this assertion. The mechanism at full saturation (1.0 mol % LiCl) was gleaned from plots showing a half-order LDA dependence (Figure 17) and zeroth-order THF dependence (Figure 18). The equilibrium approximation affords

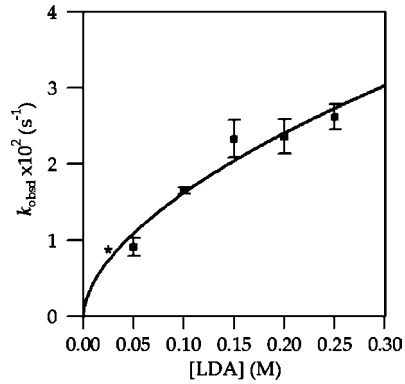

Figure 17. Plot of k_{obsd} vs [LDA] in THF (6.10 M) for the 1,4-addition of ester **1** (0.004 M) in the presence of 1 mol % LiCl at −78 °C. The curve depicts an unweighted least-squares fit to $y = k[\text{LDA}]^n$ [$k = (6.01 \pm 0.04) \times 10^{-2}$; $n = 0.57 \pm 0.08$]. The asterisk denotes a point that departed markedly from pseudo-first-order conditions and was not included in the fit.

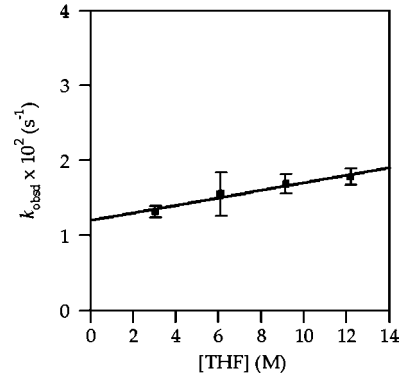

Figure 18. Plot of k_{obsd} vs [THF] in hexane cosolvent for the 1,4-addition of ester **1** (0.004 M) with LDA (0.10 M) in the presence of 1 mol % LiCl at −78 °C. The curve depicts an unweighted least-squares fit to $y = k[\text{THF}] + k'$ [$k = (5.0 \pm 0.01) \times 10^{-4}$; $k' = (1.2 \pm 0.1) \times 10^{-2}$].

the idealized[33] rate law given by eq 8, which implicates the monosolvated-monomer-based transition structure $[\text{AS(ester)}]^‡$ formed according to eq 9:[34]

$$-\frac{\text{d[ester]}}{\text{d}t} = \left(\frac{k_1}{k_{-1}}\right)^{1/2} k_2[\text{ester}][\text{S}]^0[\text{A}_2\text{S}_2]^{1/2} \qquad (8)$$

$$\text{AS} + \text{ester} \xrightarrow{k_2} [\text{AS(ester)}]^‡ \qquad (9)$$

where ester = **1**. Importantly, although LiCl catalyzes the deaggregation, it has no role in the product-determining 1,4-addition step (see eq 10 below).

We can now complete the mathematical analysis of the saturation curve in Figure 16. The transition from a rate-limiting deaggregation of dimer **3** in the absence of LiCl to a fully established pre-equilibrium at high LiCl_T concentration precludes the equilibrium approximation. The time dependencies of the concentrations of ester **1** and LDA dimer and monomer are described by eqs 10−12, respectively:

$$-\frac{\text{d[ester]}}{\text{d}t} = -k_2[\text{ester}][\text{AS}] \qquad (10)$$

(43) Espenson, J. H. *Chemical Kinetics and Reaction Mechanisms*, 2nd ed.; McGraw-Hill: New York, 1995.
(44) Frey, P. A.; Hegeman, A. D. *Enzymatic Reaction Mechanisms*; Oxford University Press: New York, 2007; Chapter 2.
(45) In fact, addition of 100 mol % LiCl causes a 3-fold *inhibition* relative to native LDA containing 1.0 mol % LiCl. Davies noted inhibition by LiCl on the 1,4-additions of chiral lithium amides to unsaturated esters (see: Davies, S. G.; Hermann, G. J.; Sweet, M. J.; Smith, A. D. *Chem. Commun.* **2004**, 1128). LiCl had no measurable effect on the stereoselectivity.

$$-\frac{d[A_2S_2]}{dt} = k_1[LiCl_T][A_2S_2] - k_{-1}[LiCl_T][AS]^2 \quad (11)$$

$$-\frac{d[AS]}{dt} = -2k_1[LiCl_T][A_2S_2] + 2k_{-1}[LiCl_T][AS]^2 + k_2[ester][AS] \approx 0 \quad (12)$$

Solving for the concentration of monomer AS in eq 12 using the quadratic equation and substituting the result into eq 10 affords the rate law in eq 13:

$$-\frac{d[ester]}{dt} = \frac{k_2[ester]}{4k_{-1}[LiCl_T]} \times \left(\sqrt{k_2^2[ester]^2 + 16k_1k_{-1}[A_2S_2][LiCl_T]^2} - k_2[ester]\right) + c \quad (13)$$

where c corresponds to the low basal rate of uncatalyzed deaggregation. The quantity $-d[ester]/dt$ in eq 13 is equal to $-(\Delta[ester]/\Delta t)_{t=0}$ obtained by initial rates. The curve in Figure 16 corresponds to a fit to eq 13. Although eq 13 lacks the intuitive appeal of simple saturation functions, the rate reduces to c as the $LiCl_T$ concentration approaches zero and to eq 8 at high $LiCl_T$ concentration.[46]

Since deaggregation is rate-limiting in the absence of LiCl (eq 3), it is logical that accelerating the deaggregation through LiCl catalysis would accelerate the reaction. Why LiCl changes the rate-limiting step is less obvious. Inspection of the mechanism in eqs 7 and 8 shows that elevated LiCl concentrations ($k_{-1}[LiCl_T] \gg k_2[ester]$) cause the reaggregation to become competitive with the 1,4-addition, eventually affording a fully established pre-equilibrium. Thus, it is formally the catalysis of the *reaggregation* of LDA monomer by LiCl that causes the 1,4-addition to become rate-limiting. Such reversibility is also required for a fractional-order dependence on LDA concentration to be observed.

The mechanism by which LiCl catalyzes the deaggregation of LDA is elusive, but a few comments are warranted. In LDA−LiCl mixtures containing low LiCl concentrations, LiCl exists exclusively as mixed aggregates **6** and **7** (1:8) to the exclusion of appreciable free LiCl.[27,28] Thus, an apparent first-order dependence on the total LiCl concentration at the lowest LiCl concentration[47] is tantamount to a first-order dependence on the mixed aggregates.

With the monosolvated-monomer-based stoichiometry established for the addition under full LiCl catalysis, we turned to DFT computations. Transition structure **10** is plausible (MP2-corrected $\Delta G^{\ddagger} = 16.3$ kcal/mol at −78 °C), although the energy is large relative to the calculated barrier for the rate-limiting deaggregation (Scheme 1).

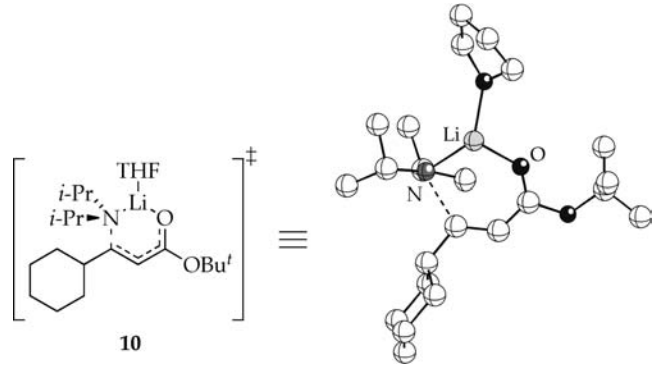

10

Competition Studies. We delineated three pathways for 1,4-addition that *may* share a common reactive intermediate: (1) uncatalyzed 1,4-addition with the key post-rate-limiting addition opaque to standard kinetic analysis; (2) autocatalyzed (enolate-mediated) deaggregation with the key 1,4-addition remaining post-rate-limiting; and (3) LiCl-catalyzed deaggregation with rate-limiting 1,4-addition (eqs 7 and 8), which was shown to proceed via LDA monomer **11**. (We have chosen to draw the fleeting monomer **11** as the computationally most stable trisolvate.[48]) Standard protocols for examining post-rate-limiting steps to probe for common (shared) intermediates usually entail comparing inter- and intramolecular isotope effects.[49] Showing that isotopic substitution affects the selectivity at a key branch point, but not the reaction rate, confirms that the isotopically sensitive step is post-rate-limiting. Since the 1,4-addition is poorly suited for isotopic labeling, we turned to a related approach using two structurally distinct substrates.

We established the reactivity of monomer **11** toward ester **1** and its *n*-alkyl analogue **12**[50] under conditions of fully saturated LiCl catalysis (eq 14):

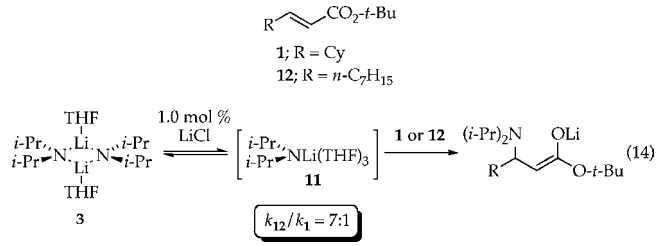

Whether in competition or in separate vessels, **12** displayed 7-fold greater reactivity. (We used gas chromatography of serially quenched separate vessels to monitor mixtures of esters **1** and **12** for the competition experiments.) The 7:1 relative reactivity provides an important benchmark for monomer **11**.

(46) Equation 13 would appear to become undefined at $[LiCl_T] = 0$, but this turns out not to be the case. Qualitatively, the $[LiCl_T]^2$ term within the argument of the square root approaches zero at low values of $[LiCl_T]$ faster than the $[LiCl_T]$ term in the denominator. Alternatively, let $a = k_2[ester]$, $b = 16k_1k_{-1}[A_2S_2]_0$, $d = 4k_{-1}$, and $x = [LiCl_T]^2$. Eq 13 can then be rewritten as

$$-\frac{d[ester]}{dt} = \frac{a}{dx^{0.5}}[(a^2 + bx)^{0.5} - a] + c = \frac{a}{dx^{0.5}}\left[a\left(1 + \frac{b}{a^2}x\right)^{0.5} - a\right] + c$$

Applying the Taylor expansion to $[1 + (b/a^2)x]^{0.5}$ for $x \ll 1$ gives

$$-\frac{d[ester]}{dt} = \frac{a}{dx^{0.5}}\left[a\left(1 + \frac{b}{2a^2}x\right) - a\right] + c = \frac{bx}{2dx^{0.5}} + c$$

Since x approaches zero faster than $x^{0.5}$, it follows that

$$\lim_{x\to 0}\left(\frac{bx}{2dx^{0.5}} + c\right) = c$$

.

(47) Although the saturation behavior is not sigmoidal, excluding a higher-order dependence on LiCl, the data do not exclude a fractional LiCl dependence.

(48) Viciu, M.; Gupta, L.; Collum, D. B. *J. Am. Chem. Soc.* **2010**, *132*, 6361.

(49) (a) Carpenter, B. K. *Determination of Organic Reaction Mechanisms*; Wiley: New York, 1984. (b) Whisler, M. C.; MacNeil, S.; Snieckus, V.; Beak, P. *Angew. Chem., Int. Ed.* **2004**, *43*, 2206.

(50) Davies, S. G.; Mulvaney, A. W.; Russell, A. J.; Smith, A. D. *Tetrahedron: Asymmetry* **2007**, *18*, 1554.

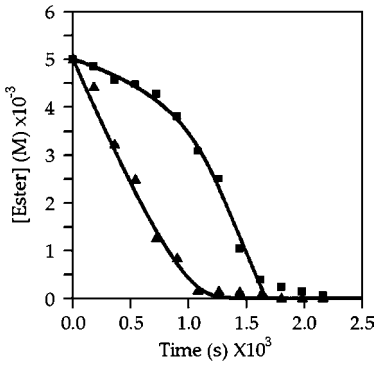

Figure 19. Plots of ester concentration vs time for the uncatalyzed 1,4-addition of LDA (0.10 M) to a mixture of esters **1** and **12** (0.005 M each) in THF (6.10 M) at −78 °C: (■) ester **1**; (▲) ester **12**. Results were analyzed by GC relative to a decane internal standard.

The uncatalyzed reaction of ester **1** with LDA involves a post-rate-limiting 1,4-addition: is the key intermediate in that case also monomer **11**? Ester **1** and *n*-alkyl analogue **12** underwent 1,4-additions at indistinguishable rates despite differing steric demands, as expected for a rate-limiting deaggregation and post-rate-limiting 1,4-addition. In contrast, reacting an equimolar mixture of **1** and **12** with 2.0 equiv of LDA revealed a 7-fold greater reactivity of **12** relative to **1** (eq 15), as expected if monomer **11** is the intermediate. We also observed that once **12** was fully consumed, ester **1** reacted at a rate comparable to that of **12** (Figure 19). Such biphasic kinetics would be expected for post-rate-limiting 1,4-additions.[51]

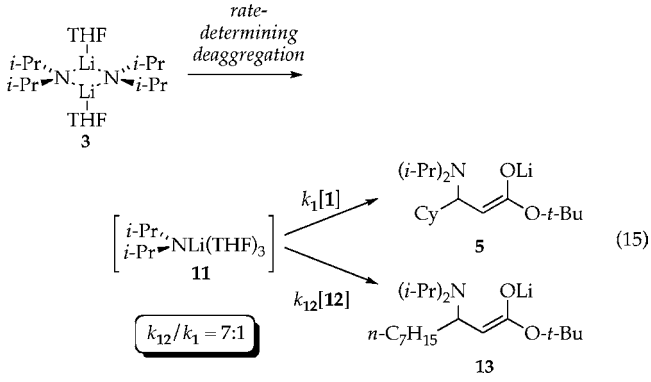

(15)

We suspected that the weak autocatalysis arises because ester enolate **5** is an inferior deaggregation catalyst in comparison with LiCl. A reaction was carried out to 50% conversion by adding 0.5 equiv of ester **1**—conditions to establish lithium enolate-induced acceleration—and subsequently treating the mixture with either **1** or **12** (separate reactions); the accelerations were indistinguishable for the two substrates. These results indicate that the formation of monomer **11** is still rate-limiting, as expected for a catalyst that is poor compared with LiCl. In contrast, treating an analogous equimolar mixture of LDA and mixed dimer **4** with an equimolar mixture of esters **1** and **12** showed a relative reactivity of 7:1. This confirmed that the back-reaction in eq 15 (the reaggregation of LDA) is slow relative to the 1,4-addition (eq 16) and showed the commonality of intermediate in the uncatalyzed and LiCl-catalyzed 1,4-additions.

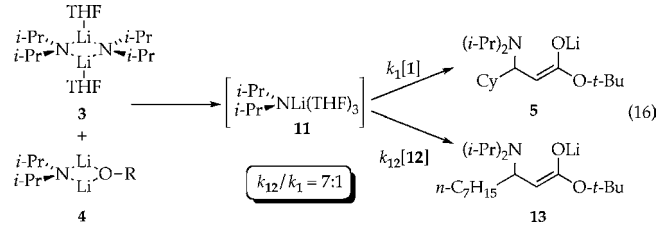

(16)

Mechanistic Hypothesis and Numerical Integrations.[52,53] The rate and mechanistic studies were pieced together to form the mechanistic hypothesis shown in Scheme 2 and described by the affiliated differential equations given in eqs 17−22. As mentioned previously, in these equations A stands for an LDA subunit and E stands for an enolate subunit. We have taken some liberties with the depiction of the model in Scheme 2 to optimize the visual presentation. Although the role of the solvent has been elucidated for a number of steps, it is not germane to the numerical fitting and has been omitted for clarity. We have depicted the critical autocatalytic step by affiliating k_3 and k_{-3} with the fleeting mixed trimer A_2E; this step is described numerically in the differential equations by means of the equilibrium $A_2 + E \rightleftarrows A + AE$. The equilibria in Scheme 2 are unbalanced to minimize clutter. However, the differential equations are all fully balanced to provide a valid mathematical description.

Scheme 2

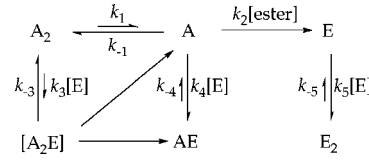

$$\frac{d[ester]}{dt} = k_2[A][ester] \quad (17)$$

$$\frac{d[A_2]}{dt} = -k_1[A_2] + k_{-1}[A]^2 - k_3[A_2][E] + k_{-3}[A][AE] \quad (18)$$

$$\frac{d[A]}{dt} = 2k_1[A_2] - 2k_{-1}[A]^2 - k_2[A][ester] + k_3[A_2][E] - k_{-3}[A][AE] - k_4[A][E] + k_{-4}[AE] \quad (19)$$

$$\frac{d[AE]}{dt} = k_3[A_2][E] - k_{-3}[A][AE] + k_4[A][E] - k_{-4}[AE] \quad (20)$$

(51) The curves in Figure 16 correspond to numerical integration of the following highly simplified model:

$$^1/_2A_2 \rightleftarrows A$$

$$A + \mathbf{1} \rightarrow \mathbf{5}$$

$$A + \mathbf{12} \rightarrow \mathbf{13}$$

$$\frac{d[E]}{dt} = k_2[A][ester] - k_3[A_2][E] + k_{-3}[A][AE] - k_4[A][E] + k_{-4}[AE] - 2k_5[E]^2 + 2k_{-5}[E_2] \quad (21)$$

$$\frac{d[E_2]}{dt} = k_5[E]^2 - k_{-5}[E_2] \quad (22)$$

It is nearly impossible to reproduce in prose how the model came into being, but we can describe the general strategy as well as the most critical constraints. We hasten to add at the outset that despite aphorisms proclaiming that anything can be fit given enough differential equations, our experience with complex systems containing a large number of restrictions and observables (see Figures 5−8) is quite the opposite. The model in Scheme 2 is the simplest model that fits the data, and many others failed to do so quite decisively.

First, a few comments about general tactics are warranted. The rate data placed significant constraints on the model. In other instances, seemingly reasonable hypotheses were excluded only through numerical simulations showing that key curvatures were not reproduced. Once the data in Figures 5−8 were qualitatively reproduced through numerical simulations, best-fit numerical integrations of eqs 17−22 afforded the functions displayed.

The key constraints imparted by the curvatures in Figures 5−8 include the following: (1) the linear decay of ester; (2) the two obvious discontinuities (most easily seen in Figure 8), namely, the maximum in enolate dimer (E_2) concentration and the marked change in the rate of formation of the mixed dimer (AE), that coincide with the consumption of ester; (3) an overshoot in the concentration of E_2 relative to the equilibrium population; and (4) the coincident formation of AE and E_2 at the outset of the reaction (most easily observed in Figure 5), indicating that AE is *not* a requisite precursor to E_2 (or vice versa).[54]

The model was assembled as follows:

(1) Rate-limiting deaggregation of A_2 gives monomer A, which subsequently reacts in a post-rate-limiting step with ester to give enolate. This enolate necessarily forms as a monomer (E). Thus, the $A_2 \rightarrow A \rightarrow E$ sequence representing the top half of Scheme 2 was fully established by traditional kinetic methods.

(2) The fate of enolate monomer E was a central issue. Self-condensation of E is one logical source of E_2 (the other logical source would be direct reaction of AE with ester). The condensation of A and E is an obvious source of the mixed dimer AE. A critical insight was that the bifurcation of E to form E_2 and AE allows for their concurrent formation (with no induction period in either case).

(3) Two factors elicited the inclusion of the pathways involving the condensation of E with A_2 (via A_2E) to give the mixed dimer AE and monomer A. (To reiterate, this was modeled as a net conversion and does not connote a single-barrier pathway.) The most important factor was that the numerical simulations failed to reproduce the curvatures. *How* the simulations failed was key, in that the simulations kept suggesting a source of AE independent of the simple reaggregation of A and E. Of course, there was considerable experimental evidence of autocatalysis, which could only arise by accelerating the rate-limiting deaggregation of LDA dimer A_2.

(4) One might ask why the autocatalytic step is depicted as proceeding via A_2E rather than through a dimer−dimer condensation via A_2E_2 that we studied kinetically. Again, the simple answer is that no amount of tinkering could force the curves to fit using an A_2E_2-based pathway. One could justify a provision for A_2E_2 *in addition to* A_2E on the basis of the kinetics of mixed aggregation described in eqs 5 and 6, but the improvement in the fit was statistically insignificant.

The components of the model in Scheme 2 are well-founded by the rate and mechanistic studies. As can be seen from Figures 5−8, the best-fit numerical integrations of eqs 17−22 are exceptional.

Discussion

It is becoming evident that reactions of LDA in THF at −78 °C are mechanistically complex even by the standards of organolithium chemistry.[11,12] Nature could not have chosen a more inauspicious opportunity—a more synthetically relevant reagent under the most commonly used conditions—to insert confusion. The complexity stems from aggregate exchanges that occur at rates comparable to those of the reaction with substrate.[10] The result is that aggregation events can become rate-limiting, and LDA-containing aggregates are not at full equilibrium on the time scales of their reactions with substrates. The first detailed investigations of such phenomena focused on ortholithiations of fluorinated aryl carbamates.[11] Almost perfectly linear decays normally attributed to zeroth-order ester dependencies were traced to the superposition of a *first*-order ester dependence and autocatalysis. In the case of the 1,4-addition, seemingly analogous linear decays were traced to the superposition of a *zeroth*-order ester dependence and much less pronounced autocatalysis. A summary of the mechanism customized for mathematical treatment is provided in Scheme 2. The more structurally illuminating version with the full complement of intermediates and transition structures is summarized in Scheme 3. A compartmentalized summary follows.

Rate-Limiting Deaggregation. Monitoring the initial rates of the uncatalyzed 1,4-addition to ester **1** revealed a true zeroth-order ester dependence: deaggregation of LDA is rate-limiting, and the 1,4-addition step is post-rate-limiting. The trisolvated-dimer-based deaggregation is either a partial deaggregation to form the open dimer[35] via transition structure **8** or a complete deaggregation to form the monomer via transition structure **9**. Computational studies indicate that **9** has the higher barrier. Even if the rate-limiting step involves formation of the open dimer via **8**, however, standard rate studies do not peer past the rate-limiting step to distinguish between the monomer-based and dimer-based reactions with ester **1**. A combination of rate studies in the presence of LiCl and competition studies (both discussed below) support monomeric intermediate **11** and monosolvated-monomer-based transition structure **10**.

Autocatalysis. The rate-limiting deaggregation of dimer **3** that is dominant at the onset of 1,4-addition is overlaid by contributions from muted autocatalysis as the reaction progresses. It is very tempting to focus on mixed dimer **4** for an explanation, but that would be wrong. Neither the elevated concentration nor higher reactivity of mixed dimer **4** causes the autocatalysis.

(52) For an explanation of Levenberg−Marquardt nonlinear least-squares optimization, see: Press, W. H.; Flannery, B. P.; Teukolsky, S. A.; Vetterling, V. T. *Numerical Recipes in C*; Cambridge University Press: London, 1988; Chapter 14.4.

(53) Brown, P. N.; Byrne, G. D.; Hindmarsh, A. C. *J. Sci. Stat. Comput.* **1989**, *10*, 1038.

(54) Given a reaction coordinate SM → I → P in which I builds to appreciable concentrations, the rate of formation of P will show an induction period (see ref 43).

Scheme 3

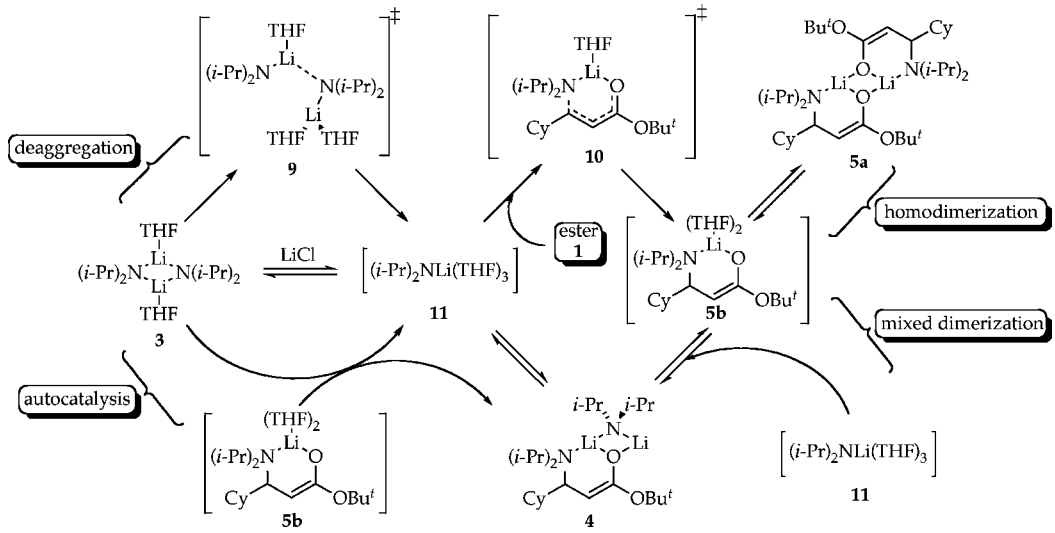

Mixed dimer **4** could react with ester **1** instantaneously, and this *still* would not constitute autocatalysis. An autocatalyst *must* catalyze the rate-limiting deaggregation of LDA. To understand the autocatalysis, it is instructive to focus on the structurally simplified model in Scheme 2.

Autocatalysis stems from acceleration of the rate-limiting deaggregation of LDA dimer, denoted as A_2. Notably, enolate homodimer E_2 is an ineffectual catalyst: it reacts with LDA dimer *very* slowly. The autocatalysis was traced to the reaction of enolate *monomer* E. When LDA monomer A reacts with ester to form enolate monomer E, E can dimerize to form E_2 or react with an LDA monomer A to form the mixed dimer AE. Occasionally, however, E reacts with LDA dimer A_2 to form AE and monomer A. *This* is autocatalysis.

The data, however, seem paradoxical. The plot of the reaction rate versus time when equimolar LDA and ester were used (Figure 4) shows some straightening that hints at autocatalysis, but a marked sigmoidal decay characteristic of virulent autocatalysis is notably absent. In short, the reaction is *not* faster at 50% conversion. In contrast, however, incremental additions of ester **1** to LDA (Figure 13) showed a marked increase in rate with each increment, reaching a net 4-fold higher rate at 50% consumption of LDA and 50% formation of enolate. An analogous 4-fold autocatalysis certainly would have elicited a quite distinct sigmoidal curvature in Figure 4.

How do we reconcile these two contrasting views? The key to understanding Figure 13 is to note that under normal reaction conditions, the aggregates are *not* at full equilibrium, so the LDA−enolate mixed dimer AE remains well below its equilibrium concentration. In contrast, the incremental additions in Figure 13 allow full equilibration of the aggregates between increments. As a consequence, AE attains substantial equilibrium concentrations. When the subsequent increment of ester is added, the key LDA monomer is generated either from rate-limiting deaggregation of A_2 or by a more facile (and only partially rate-limiting) deaggregation of mixed dimer AE. The rate maximum in Figure 13 corresponds to the maximum concentration of the kinetically labile AE mixed dimer. Thus, an experiment initially intended to explicitly probe autocatalysis uncovered an altogether different mixed aggregation effect. We will return to these distinctions below.

LiCl Catalysis. The 1,4-addition of LDA to ester **1** is measurably accelerated by as little as 0.001 mol % LiCl (i.e., *1.0 ppm*). At the risk of stating the obvious, we note that this is remarkably efficient catalysis.[13] Readers might be unsurprised that this catalysis plagued the rate studies until we adapted protocols for preparing rigorously LiCl-free LDA from lithium metal.[20] (Ironically, the modified synthesis is also more convenient than our standard method.)

Lithium chloride accelerates the 1,4-addition by catalyzing the deaggregation of LDA, as summarized in eqs 7 and 8. Saturation behavior (Figure 16) with an onset of saturation at >0.5 mol % LiCl derives from a LiCl-catalyzed exchange of LDA dimers and monomers, resulting in a change from rate-limiting deaggregation to rate-limiting 1,4-addition. How LiCl catalyzes LDA deaggregation is still unclear and the subject of ongoing investigations. Nonetheless, the rate studies revealed a monosolvated monomer-based pathway for the addition, and the computational studies filled in the intimate details of transition structure **10**.

Competition Studies: Commonality of Intermediate. Competing esters **1** and **12** having different steric demands allowed us to probe the post-rate-limiting reactivity (eqs 14−16). These studies are tactically analogous to comparisons of inter- and intramolecular isotope effects.[50]

The substrate-dependent rates under LiCl catalysis showed that the 1,4-addition is rate-limiting. Ester **12** is 7 times more reactive than ester **1** toward monomer **11** (eq 14) both in separate reactions and in competition. Most importantly, this 7:1 preference serves as a benchmark for the monomer-based addition.

In the 1,4-addition under *uncatalyzed* conditions, where partial or total deaggregation is rate-limiting, the rates of 1,4-addition were identical for **1** and **12** when measured independently, confirming a post-rate-limiting addition. Using mixtures of **1** and **12** in competition, however, produced the same 7-fold higher reactivity of **12** (eq 15) characteristic of trapping of monomer **11**.

A competition was carried out using equimolar mixtures of LDA and lithium enolate **5** to examine the influence of mixed dimer **4** (eq 16). When compared independently, esters **1** and **12** showed identical reactivities, indicating that the deaggregations of **3** *and* **4** remain rate-limiting. In contrast, competition of **1** and **12** revealed the 7-fold greater reactivity of **12** characteristic of reaction with monomer **11**.

Do the 7:1 selectivities for the uncatalyzed, LiCl-catalyzed, and enolate-mediated additions *rigorously* show the commonal-

ity of intermediate **11** and transition structure **10**? In a word, no. The selectivities do, however, make for a compelling circumstantial case.

Mixed Aggregation Effects: Four Variants. Effects of lithium salts on organolithium reactivity—so-called mixed aggregation effects—were first documented decades ago.[14] Examples of mixed aggregation effects on rates and selectivities, whether LiX salts are added explicitly or formed in situ, are now legion.[13] Mechanistically well-defined examples, however, are quite rare by comparison.[15] We take this opportunity to discuss four distinct classes of mixed aggregation effects using LDA emblematically.

Case 1. Probably the most often cited and certainly the most intuitively simple salt effect derives from the direct reaction of mixed aggregates (such as **4**, **6**, and **7**) with substrate (eq 23). Because the steric and electronic properties of LDA−LiX mixed aggregates are markedly different than those of homoaggregated LDA dimer **3** and the LiX salt is assumed to be strategically located in the rate- and product-determining transition structures, it is easy to understand how LiX could markedly influence both the rate and selectivity. We have documented the direct reaction of LDA mixed dimers.[15] Although the mixed aggregates could be either fleetingly stable or observable quantitatively, inhibition by observable mixed aggregates is prevalent.[15,55] The critical requirement common to all examples in case 1, whether inhibiting or accelerating, is that the LiX salt remain intimately involved in the rate- or product-determining transition structure.

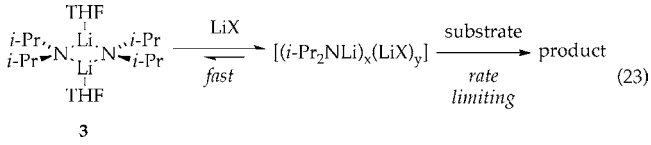

3 (23)

Case 2. Rate reductions are not the only consequence of inhibition. Imagine that a mixed aggregate forms quantitatively and shows no reactivity toward substrate (eq 24). The only available avenue of reaction is via free LDA. To the extent that the steady-state concentration of LDA is decreased to very low levels, representing a dilution of sorts, monomer-based pathways will be promoted relative to dimer-based pathways.[56] The influence of such a mass-action effect on the efficacies of the monomer- and dimer-based pathways is illustrated in eq 25.[15] Indeed, an LDA-dimer-based ester enolization was diverted by an intervening LDA−lithium enolate mixed dimer through both mixed-dimer-based *and* monomer-based pathways. To the extent that LiX can divert a dimer-based pathway to a monomer-based pathway, an LiX-dependent change in selectivity could arise *without intimate association of LiX with the product-determining transition structure*.

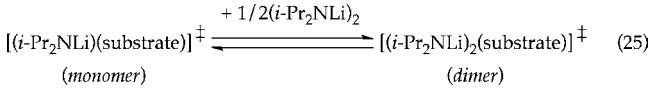

(25)

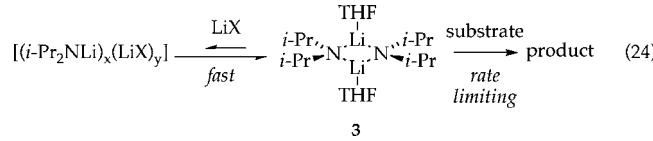

3 (24)

Case 3. The mixed aggregation effects described in this paper involve LiX-catalyzed deaggregation. We must point out that there is jargon in the literature that loosely refers to LDA−LiX mixed aggregates as deaggregated because the mixed aggregate contains only one LDA subunit. We find this usage to be unconstructive. In the case described herein, however, the role of LiX salts (LiCl and, to a much lesser extent, lithium enolate) is to catalyze the formation of true LDA monomer (eq 26). To the best of our knowledge, this catalysis is undocumented. It could be observed only for reactions in which deaggregation is either rate-limiting or precluded altogether by a high barrier (forcing the reaction to occur with the aggregated form). No catalysis by LiCl will be observed if all of the aggregation states fully equilibrate on the time scale of the reaction without added catalyst. Of course, to the extent that a rate-limiting deaggregation is accelerated, the overall reaction will be accelerated also. If that catalysis affords the same intermediate as the uncatalyzed deaggregation (monomer **11**), only faster, then the accelerations and even changes in the rate-limiting step will *not* be accompanied by changes in regio- or stereoselectivity. However, if the preferred pathway for the uncatalyzed reaction is *dimer*-based because of a prohibitively high barrier to deaggregation and LiX catalyzes monomer formation, the acceleration could be accompanied by a change in selectivity. We suspect that regioselective ortholithiations may be a fruitful place to look for such phenomena.

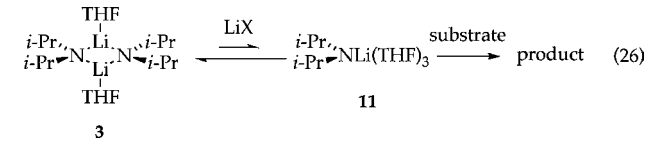

3 11 (26)

Case 4. In cases 1 and 2, we have implicitly assumed that the aggregate exchanges are fast relative to reactions with substrate. Under this criterion, mixed aggregation must necessarily inhibit a reaction according to the principle of detailed balance[56] unless the mixed aggregate can react with the substrate directly and rapidly. Case 4 addresses the consequences of mixed aggregation when aggregate exchanges are *not* at equilibrium during the course of the reaction. If, for example, deaggregations of LDA dimer **3** and mixed dimer **4** are rate-limiting (i.e., if the reaction with LDA monomer is at least competitive with reaggregation, as the model in Scheme 2 suggests), the result would be a scenario in which facile deaggregation of mixed dimer **4** increases the rate that monomeric LDA is released and subsequently trapped. Formally, this is not autocatalysis because autocatalysis requires a provision for accelerating the deaggregation of LDA dimer **3**. Solutions containing considerable concentrations of labile mixed dimer **4**, however, would show a higher reactivity than analogous solutions containing only LDA dimer **3**. This scenario accounts for 1,4-additions in the presence of enolate that are more rapid than would be predicted on the basis of the low levels of autocatalysis.

Conclusion

A number of consequences of the work described herein are clear. Because traces of LiCl may contaminate LDA, source

(55) (a) Sun, X.; Collum, D. B. *J. Am. Chem. Soc.* **2000**, *122*, 2459. (b) See the references cited in ref 6.

(56) The principle of detailed balance asserts that individual equilibria within an ensemble of equilibria are maintained.[57b−d] It is particularly useful in understanding the complex equilibria observed in organolithium chemistry. See: (a) Alberty, R. A. *J. Chem. Educ.* **2004**, *81*, 1206–1209. (b) Casado, J.; Lopez-Quintela, M. A.; Lorenzo-Barral, F. M. *J. Chem. Educ.* **1986**, *63*, 450. (c) Hammes, G. G. *Principles of Chemical Kinetics*; Academic Press: New York, 1978; pp 14−15.

and batch dependencies could become acute. Synthetic chemists carrying out LDA-mediated reactions in THF at −78 °C might notice enormous differences between commercial LDA (which tends to be LiCl-free) and LDA generated in situ from *n*-BuLi (which contains ample LiCl to catalyze exchanges). Indeed, this is the case for the 1,4-addition in eq 1. Adding traces of LiCl (in the form of Et_3NHCl) to commercial LDA equalizes the two protocols. Moreover, marked catalysis by traces of LiCl and inhibitions by molar excesses of LiCl suggest that the quantity of LiCl is important. We are reminded of LDA-mediated 3-pentanone enolizations, in which the *E*/*Z* selectivities are maximized using fractional-equivalent amounts of LiCl.[28] Could a composite of mixed aggregation effects be operative? We have long believed that deconvoluting the roles of LiCl in *E*-selective ketone enolizations would remain outside our grasp, but we are not so pessimistic now. We have also reported LiCl-accelerated ortholithiations in which traces of LiCl dramatically accelerated the rates but had *no* influence on regiocontrol because the regioisomers were fully equilibrated.[57] Some LDA-mediated ortholithiations are *not* at equilibrium,[58] however, and may display regioselectivities that *are* sensitive to traces of LiCl.

It is instructive to look forward. We have now reported two extensive studies of LDA-mediated reactions in which inordinate complexity rears its ugly head under conditions favored by synthetic chemists: LDA/THF/−78 °C. This is no bizarre coincidence: under these conditions, aggregation events occur with half-lives on the order of minutes. *Any* LDA/THF-mediated reaction that proceeds on a similar time scale at −78 °C will be subjected to potentially rate-limiting deaggregation and display a hypersensitivity to added lithium salts. Subtle changes in substrate reactivity and product (autocatalyst) structure could cause marked shifts in the relative efficacies of the competing steps and consequent baffling changes in rate behavior. Ongoing studies suggest that there may even be several rate-limiting LDA deaggregations (depending on the choice of substrate) and several variants of autocatalysis. We are becoming increasingly certain that many—possibly all—LDA/THF-mediated reactions carried out at −78 °C are influenced by the rates at which aggregates exchange.

We close with a caveat, but not one readers may expect. In the earliest studies of organolithium chemistry, when the role of mixed aggregates was beginning to surface, salt effects were often couched in a mechanistic context and language that were inadequate. Chastened by that experience and the daunting mechanistic and structural complexity, specialists often warn nonspecialists against invoking overly simplistic interpretations of salt effects on organolithium rates and selectivities. We admit some schadenfreude when uncovering complexity that undermines conventional mechanistic views, but it would be unfortunate if speculation (even unsubstantiated speculation) becomes stifled.

Experimental Section

Reagents and Solvents. THF and hexanes were distilled from blue or purple solutions containing sodium benzophenone ketyl. The hexanes contained 1% tetraglyme to dissolve the ketyl. Esters **1** and **12** were prepared via literature protocols.[22,50] Et_3NHCl was recrystallized from THF/2-propanol.

Preparation and Purification of LDA. Modifications of literature procedures[20] were used to prepare LDA as a LiCl-free and ligand-free solid as follows. A 250 mL Schlenk flask with an attached fine-mesh glass frit and a 250 mL receiving flask was charged with lithium shavings (1.11 g, 160 mmol), diisopropylamine (16.5 g, 160 mmol), and 80 mL of Me_2NEt. The flask was submerged in a bath at 25 °C, and isoprene (5.44 g, 80 mmol) in 30 mL of dry Me_2NEt was added over 1.0 h via syringe pump. The solution was stirred for 1.0 h at 25 °C until the lithium dissolved. (The reaction became exothermic when isoprene was added too quickly, affording highly undesirable dark-yellow or purple solutions if the temperature exceeded 35 °C.) The nearly homogeneous reaction mixture was filtered through a fine-mesh glass frit, and the solvent was removed under vacuum (∼6 h) to afford LDA as a white solid (16.0 g, 90% yield). With the aid of a glovebox, the LDA (8.0 g) was transferred to a 250 mL round-bottom flask fitted with a fine-mesh glass frit and a 250 mL pear-shaped receiving flask fitted with a side arm/stopcock. The apparatus was attached to a vacuum line, and ∼200 mL of hexanes was vacuum-transferred into the flask containing the solid LDA. The slurry was stirred at 63 °C for ∼2 h to afford a pale-yellow solution of LDA that was subsequently filtered to remove any undissolved particles. The filtrate was transferred by cannula to a 250 mL round-bottom flask fitted with a coarse-mesh glass frit and a 250 mL receiving flask. The solution was cooled to −78 °C by incrementally raising a dry ice/acetone bath to precipitate the LDA and held at −78 °C overnight. The mother liquor was carefully removed by filtration, and the solid was washed three times with 10 mL of hexanes and then dried in vacuo for 6 h. The assembly was moved to the glovebox, where the LDA was collected as a white solid in 75−85% yield. The isolated material was spectroscopically indistinguishable from samples prepared previously.[18]

Synthesis of 2. Unsaturated ester **1** (0.63 g, 3.0 mmol) in 3.0 mL of THF was added to LDA (0.64 g, 6.0 mmol) in 15 mL of THF at −78 °C. The solution was stirred for 30 min and then warmed to room temperature with stirring for 1.0 h. The reaction was quenched with 10 mL of H_2O, and the mixture was extracted with diethyl ether (3 × 10 mL). The extracts were dried using Na_2SO_4, and the solvent was removed in vacuo. The residue was redissolved in CH_2Cl_2 (5 mL) and extracted with 4.0 M HCl (3 × 3 mL). The aqueous layer was neutralized with 10% NaOH and extracted with diethyl ether (3 × 5 mL). The combined organic layers were dried with $MgSO_4$, and the solvent was removed. Flash chromatography (30% ethyl acetate/hexane) afforded amino ester **2** (78−82% yield) having the spectral properties described previously.[5]

IR Spectroscopic Analyses. IR spectra were recorded using an in situ IR spectrometer fitted with a 30-bounce silicon-tipped probe. The spectra were acquired in 16 scans at a gain of 1 and a resolution of 4 cm^{-1}, and the absorbance at 1715 cm^{-1} was monitored over the course of the reaction. For the most rapid reactions, IR spectra were recorded every 3 s.

A representative reaction was carried out as follows: The IR probe was inserted through a nylon adapter and O-ring seal into an oven-dried, cylindrical flask fitted with a magnetic stir bar and a T-joint. The T-joint was capped by a septum for injections and a nitrogen line. After the flask was evacuated under full vacuum, heated, and flushed with nitrogen, it was charged with LDA (107 mg, 1.00 mmol) in THF and cooled in a dry ice/acetone bath

(57) (a) Cottet, F.; Schlosser, M. *Eur. J. Org. Chem.* **2004**, 3793. (b) Trecourt, F.; Mallet, M.; Marsais, F.; Quéguiner, G. *J. Org. Chem.* **1988**, *53*, 1367. (c) Comins, D. L.; LaMunyon, D. H. *Tetrahedron Lett.* **1988**, *29*, 773. (d) Eaton, P. E.; Cunkle, G. T.; Marchioro, G.; Martin, R. M. *J. Am. Chem. Soc.* **1987**, *109*, 948. (e) Bridges., A. J.; Patt, W. C.; Stickney, T. M. *J. Org. Chem.* **1990**, *55*, 773. (f) Trécourt, F.; Marsais, F.; Güngör, T.; Quéguiner, G. *J. Chem. Soc., Perkin Trans. 1* **1990**, 2409. (g) Gros, P. C.; Fort, Y. *Eur. J. Org. Chem.* **2009**, 4199. (h) Cottet, F.; Marull, M.; Lefebvre, O.; Schlosser, M. *Eur. J. Org. Chem.* **2003**, 1559. (i) Güngör, T.; Marsais, F.; Queguiner, G. *J. Organomet. Chem.* **1981**, *215*, 139.

(58) (a) Schlosser, M. *Angew. Chem., Int. Ed.* **2005**, *44*, 376. (b) Schlosser, M.; Rausis, T. *Eur. J. Org. Chem.* **2004**, 1018.

prepared from fresh acetone. LiCl (0.5 mol % relative to LDA) was added as a stock solution (0.50 mL) containing $Et_3N \cdot HCl$ (8.3 mg, 0.06 mmol) and LDA (13.5 mg, 0.12 mmol) in 5 mL of THF. After recording a background spectrum, we added ester **1** (0.005 mmol) with stirring.

NMR Spectroscopic Analyses. All of the NMR tubes were prepared using stock solutions and sealed under partial vacuum. Standard ^{6}Li, ^{13}C, and ^{15}N NMR spectra were recorded on a 500 MHz spectrometer at 73.57, 125.79, and 50.66 MHz, respectively. The ^{6}Li, ^{13}C, and ^{15}N resonances were referenced to 0.30 M [^{6}Li]LiCl/MeOH at −90 °C (0.0 ppm), the CH_2O resonance of THF at −90 °C (67.57 ppm), and neat Me_2NEt at −90 °C (25.7 ppm), respectively.

Numerical Integrations. The time-dependent concentration plots obtained using ^{6}Li NMR spectroscopy (Figures 5−8) were fit to a mechanistic model expressed by a set of differential equations. The curve fitting minimized χ^2 in searching for the coefficient values (rate constants). The Levenberg−Marquardt algorithm[52] used for the χ^2 minimization is a form of nonlinear least-squares fitting. The fitting procedure implemented numerical integration based on the backward-differentiation formula[53] to solve the differential equations, yielding functions describing concentration versus time.

Acknowledgment. We thank the National Institutes of Health (GM39764 and, in part, GM 077167) for direct support of this work and Pfizer, Merck, and Sanofi-Aventis for indirect support.

Supporting Information Available: NMR, rate, and computational data; experimental protocols; details of the numerical integrations; and complete ref 25. This material is available free of charge via the Internet at http://pubs.acs.org.

JA105855V